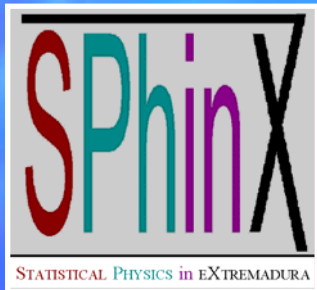


The Penetrable-sphere model: A fluid of ghost particles



Andrés Santos*
University of Extremadura
Badajoz, Spain



* In collaboration with Luis Acedo (Badajoz)
and Alexander Malijevský (Prague)

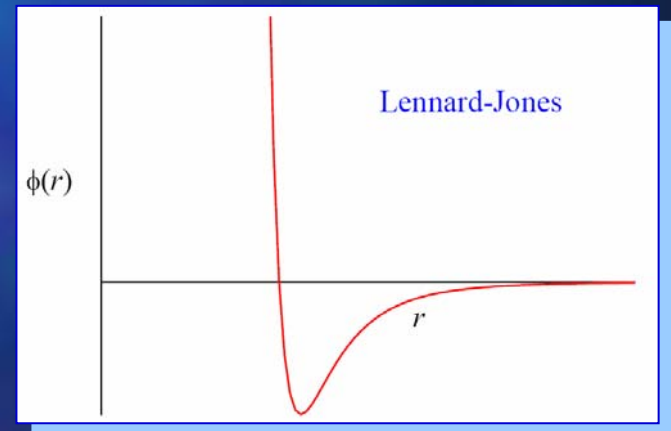
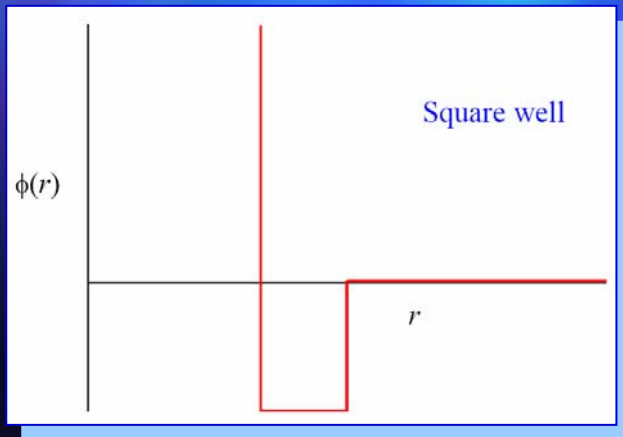
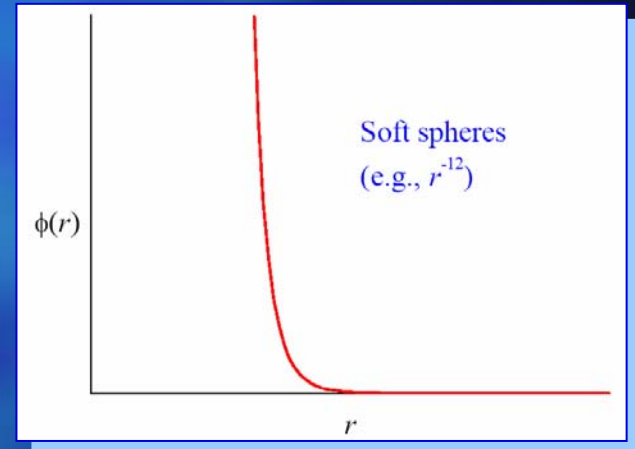
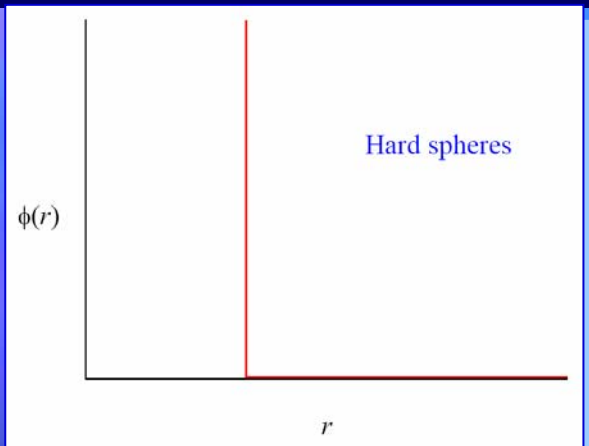
Outline

- Effective interactions in colloidal dispersions. The penetrable-sphere (PS) model.
- A few (general) statistical-mechanical definitions.
- Exact properties of the PS fluid in the high-temperature limit. Spinodal instability.
- The high-T approximation.
- The low-T approximation (1D).
- Comparison with MC simulations (1D).
- Conclusions.

Outline

- Effective interactions in colloidal dispersions. The penetrable-sphere (PS) model.
- A few (general) statistical-mechanical definitions.
- Exact properties of the PS fluid in the high-temperature limit. Spinodal instability.
- The high-T approximation.
- The low-T approximation (1D).
- Comparison with MC simulations (1D).
- Conclusions.

Traditionally, equilibrium statistical mechanics is applied to particles interacting via *unbounded* potentials, e.g.,



Unbounded potentials are useful representations of the interactions in *atomic* systems, as well as in some *colloidal* dispersions.

For instance, the effective interaction between two sterically stabilized colloidal particles is essentially HS, perhaps with a short-range attraction (depletion effects)

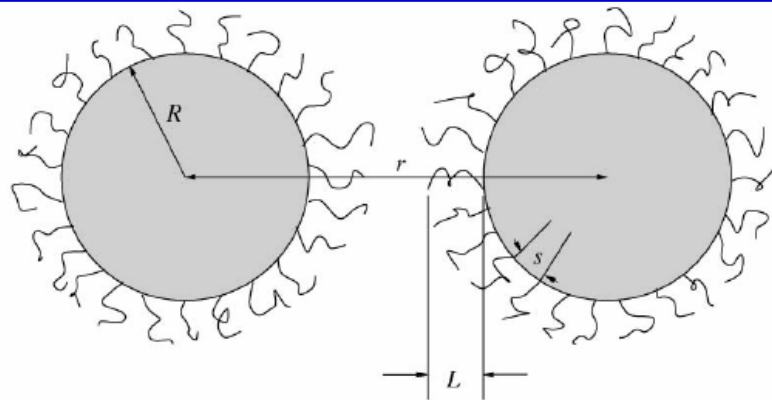


Fig. 4. Two sterically stabilized colloidal particles, each being covered with a polymeric brush whose height is L . The distance between neighboring anchored chains is denoted by s .

C.N. Likos / Physics Reports 348 (2001) 267–439

On the other hand, the effective interaction for *star polymers* in good solvents is ultrasoft, logarithmically diverging for short distances.

C.N. Likos / *Physics Reports* 348 (2001) 267–439

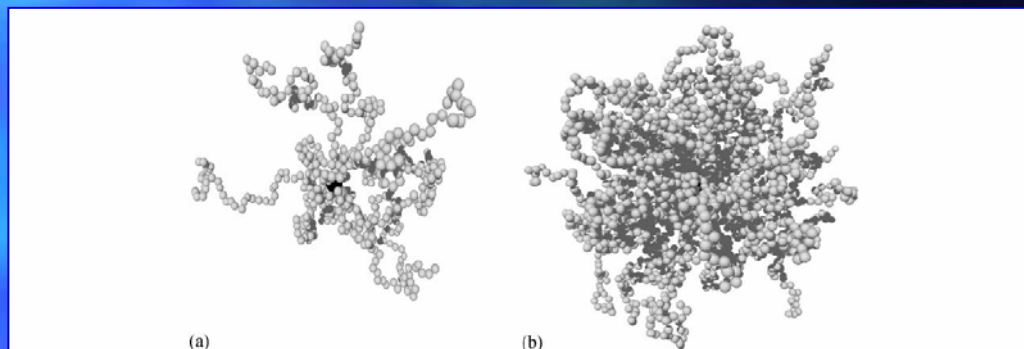


Fig. 37. Snapshots of star polymers in good solvents as obtained from MD simulations employing the model of Grest et al. [330] with: (a) $f = 10$, $N = 50$, and (b) $f = 50$, $N = 50$. For small f , the star looks like a fractal, aspherical object whereas for large f it resembles a spherical colloidal particle. (Taken from Ref. [331].)

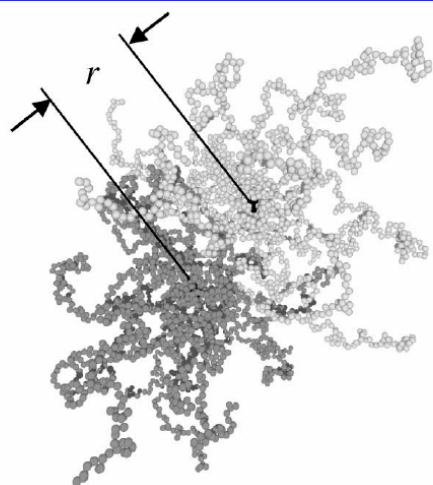


Fig. 42. Typical configuration for two stars with $f = 30$ and $N = 50$, as obtained from a simulation of Ref. [78], with r denoting the distance between their centers. (Courtesy of Art)

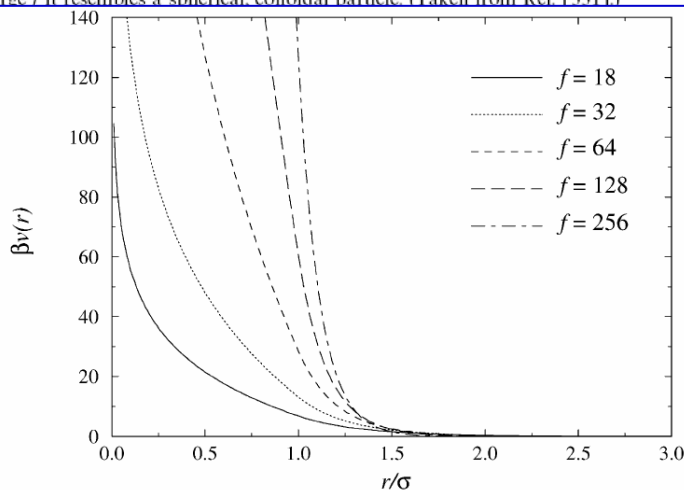


Fig. 40. The effective star-star potential of Eq. (5.57) for a number of different f -values. Notice that the potential becomes harder with increasing f , tending eventually to a HS interaction for $f \rightarrow \infty$.

Dilute solution of *polymer chains* in a good solvent

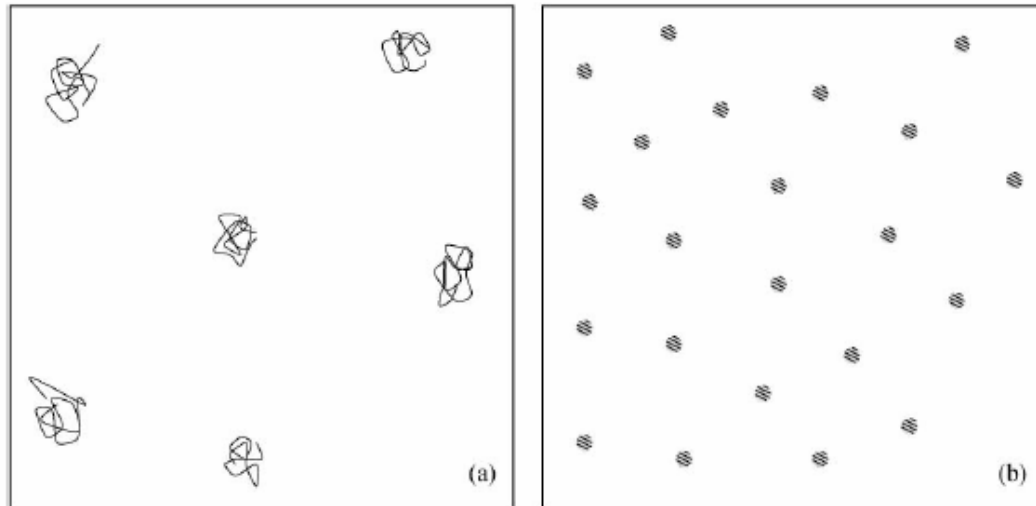


Fig. 13. A dilute polymer solution observed through two different microscopes. In (a) the microscope can resolve details above the monomer length whereas in (b) the microscope can only resolve details above the size of the chain. As a result, all length scales in (b) appear reduced with respect to those in (a) and the objects which appear as flexible chains in (a) show up as “point particles” in (b). Note that the field of view in (b) includes many more particles than in (a).

C.N. Likos / Physics Reports 348 (2001) 267–439

Two polymer chains can “sit on top of each other”

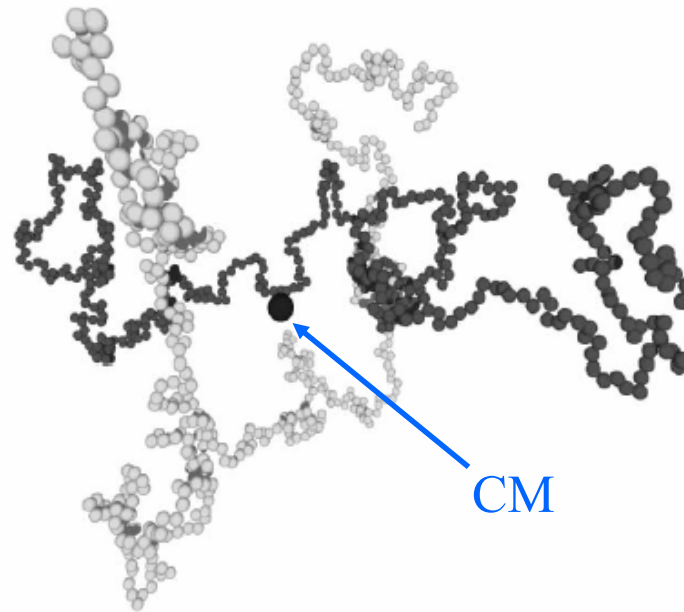
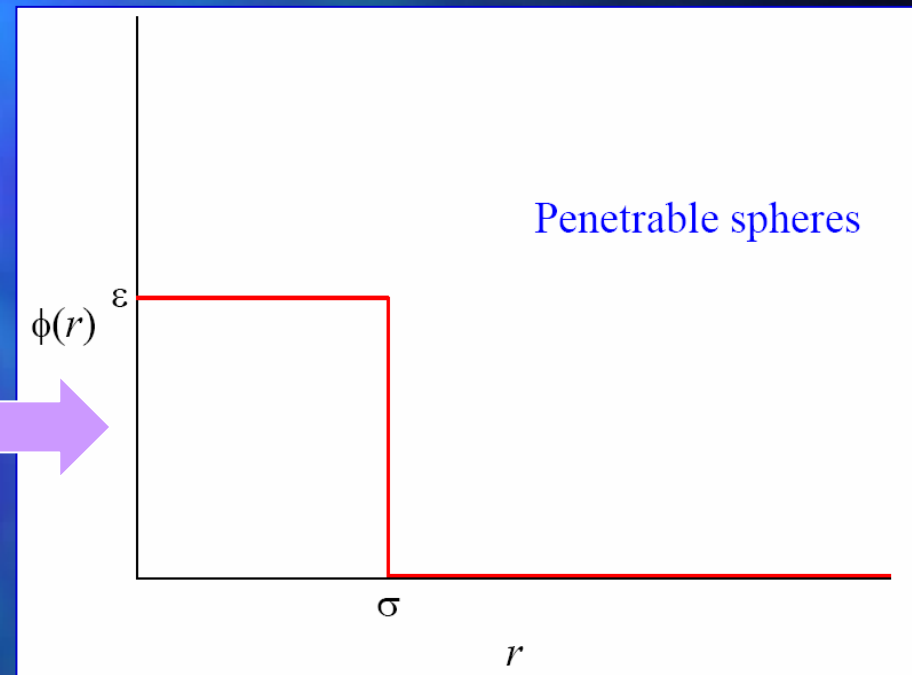
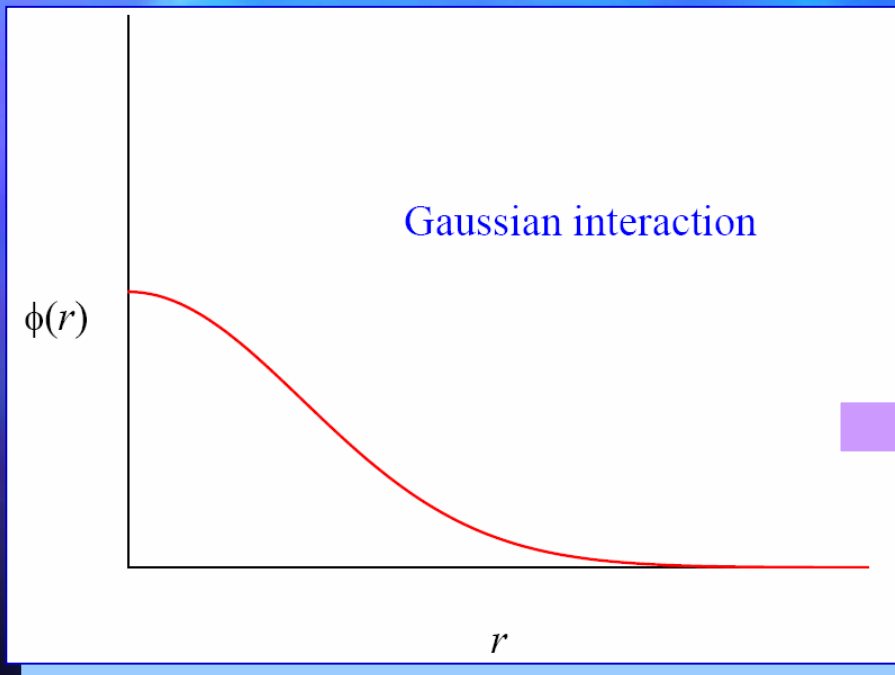


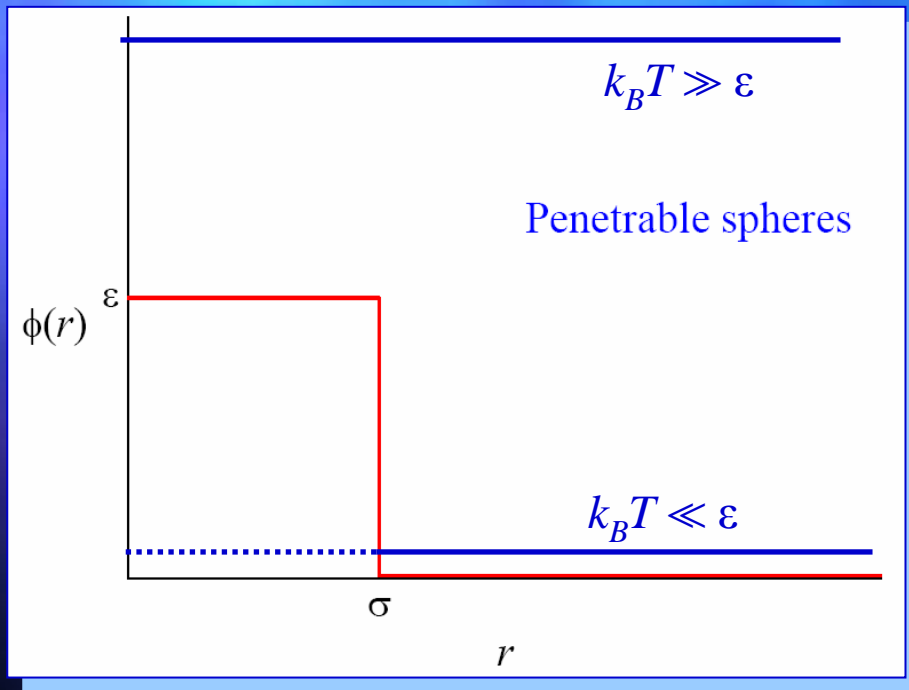
Fig. 14. A snapshot from a simulation involving two self-avoiding polymers. In this configuration, the centers of mass of the two chains (denoted by the big sphere) coincide, without violation of the excluded-volume conditions. (Courtesy of Arben Jusufi.)

C.N. Likos / Physics Reports 348 (2001) 267–439

Effective interaction between two polymer chains in a good solvent:



Aim: To obtain *analytical* approximations for the (equilibrium) structural properties of a PS fluid



$$T^* \equiv k_B T / \varepsilon$$

$T^* \rightarrow \infty$: ideal gas

$T^* \rightarrow 0$: hard-sphere fluid

Outline

- Effective interactions in colloidal dispersions. The penetrable-sphere (PS) model.
- A few (general) statistical-mechanical definitions.
- Exact properties of the PS fluid in the high-temperature limit. Spinodal instability.
- The high-T approximation.
- The low-T approximation (1D).
- Comparison with MC simulations (1D).
- Conclusions.

A few definitions (homogeneous fluid):

$\rho_2(\mathbf{r}_1, \mathbf{r}_2) = \rho^2 g(|\mathbf{r}_1 - \mathbf{r}_2|)$; $g(r)$: radial distribution function

$y(r) = e^{\phi(r)/k_B T} g(r)$: cavity function

$h(r) = g(r) - 1$: total correlation function

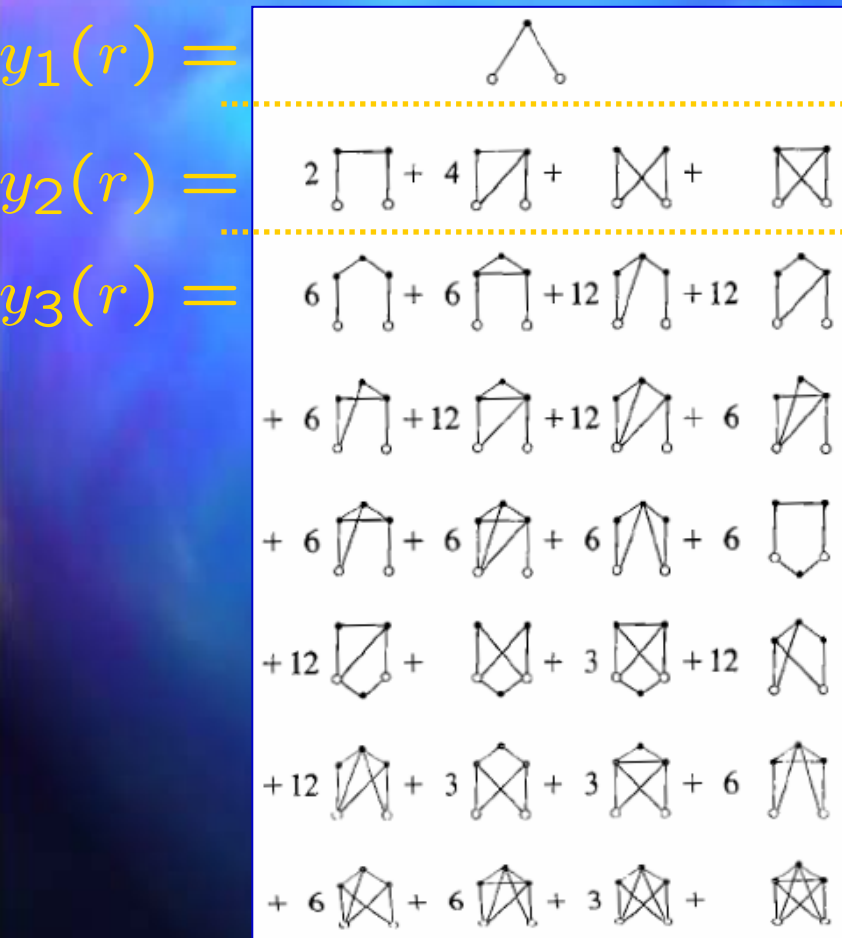
$c(r)$: direct correlation function

$\tilde{c}(k) = \frac{\tilde{h}(k)}{1 + \rho \tilde{h}(k)}$: Ornstein–Zernike relation

$S(k) = 1 + \rho \tilde{h}(k)$: structure factor

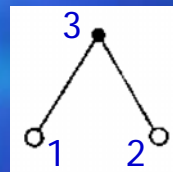
Expansion of the radial distribution function in powers of density

$$y(r) \equiv g(r) = 1 + \sum_{n=1}^{\infty} \frac{\rho^n}{n!} y_n(r)$$

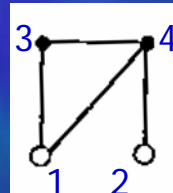


$$f(r) = e^{-\phi(r)/k_B T} - 1$$

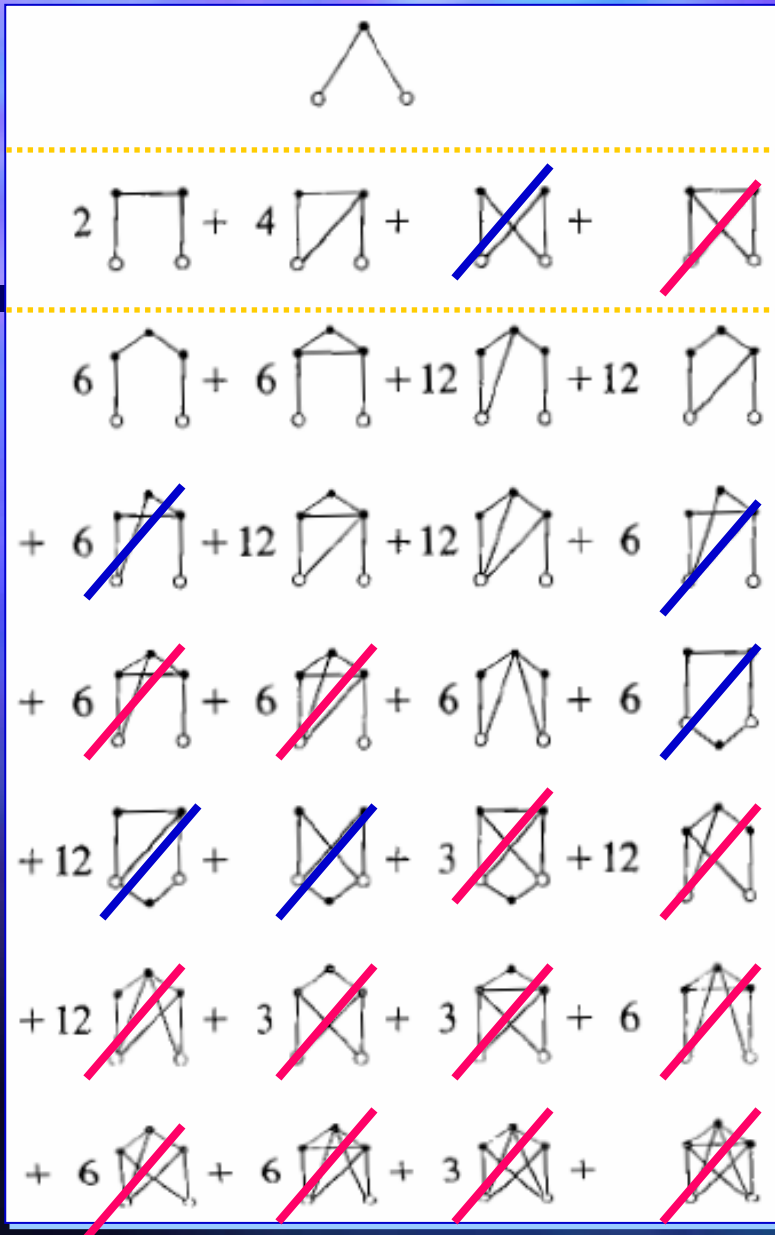
Mayer function



$$= \int dr_3 f(r_{13}) f(r_{23})$$



$$= \int dr_3 \int dr_4 f(r_{13}) f(r_{34}) \times f(r_{24}) f(r_{14})$$



HNC closure:

$$c(r) = g(r) - 1 - \ln y(r)$$

"Elementary" diagrams neglected

Percus–Yevick closure:

$$c(r) = g(r) - y(r)$$

"Elementary" and "Bundle" diagrams neglected

Freezing and clustering transitions for penetrable spheres

C. N. Likos,¹ M. Watzlawek,² and H. Löwen^{1,2}

3D

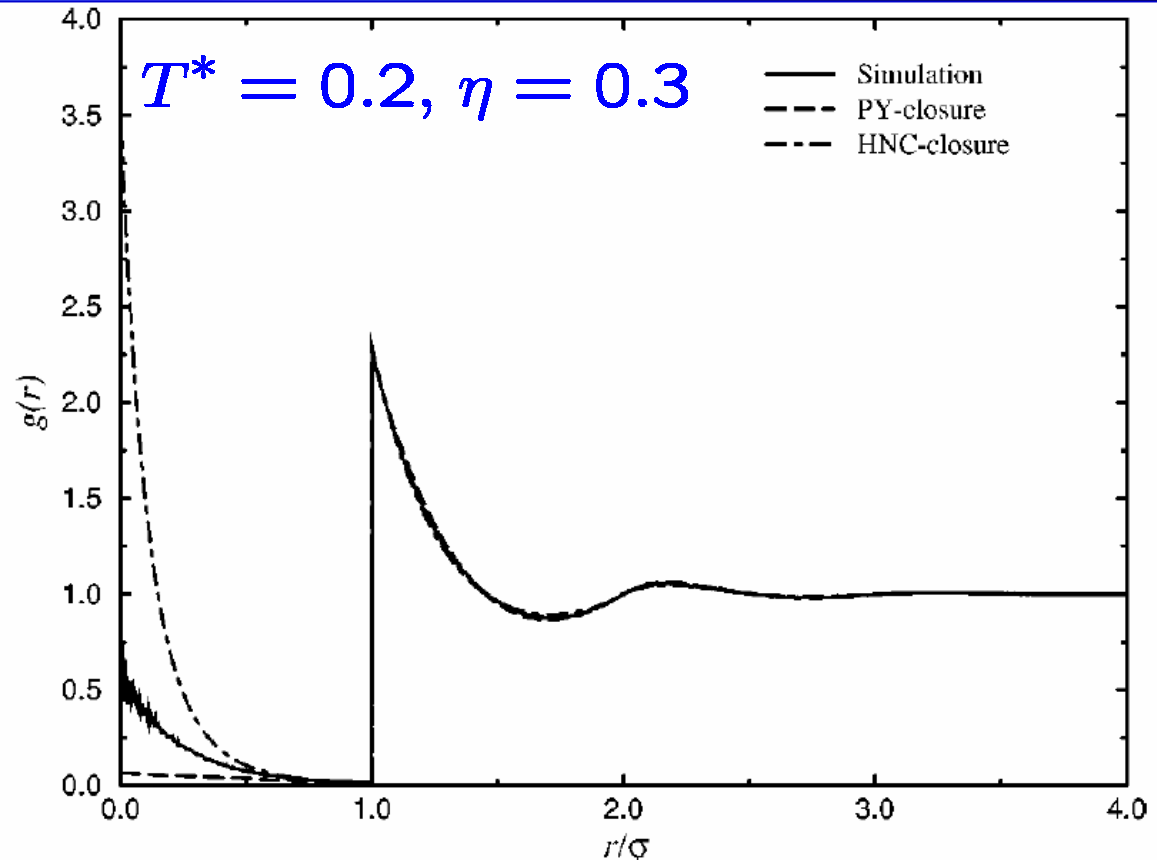


FIG. 1. Comparison of the radial distribution function $g(r)$ as obtained from simulation, and the PY and HNC closures, for a system of penetrable spheres at reduced temperature $t=0.2$ and packing fraction $\eta=0.3$.

Outline

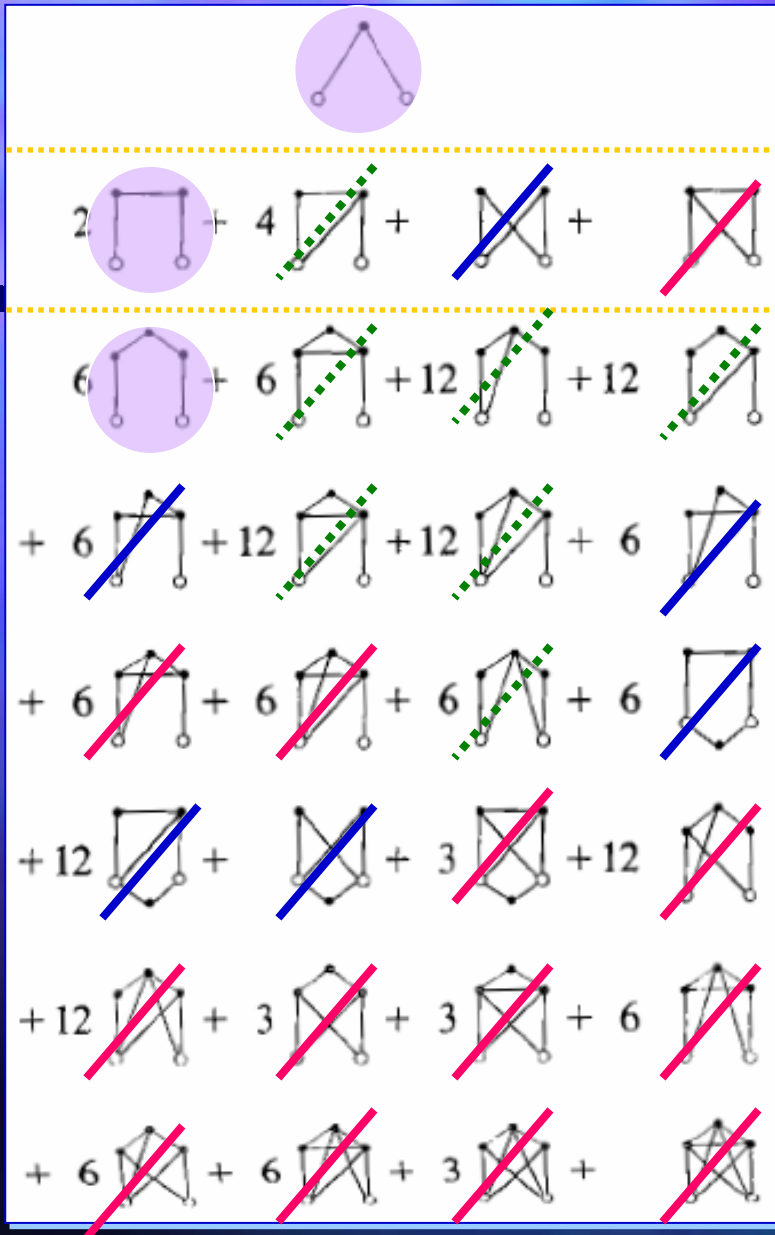
- Effective interactions in colloidal dispersions. The penetrable-sphere (PS) model.
- A few (general) statistical-mechanical definitions.
- Exact properties of the PS fluid in the high-temperature limit. Spinodal instability.
- The high-T approximation.
- The low-T approximation (1D).
- Comparison with MC simulations (1D).
- Conclusions.

Mayer function of the PS model

$$f_{\text{PS}}(r) = x f_{\text{HS}}(r), \quad x \equiv 1 - e^{-1/T^*}$$

$$f_{\text{HS}}(r) = \begin{cases} -1, & r < \sigma \\ 0, & r > \sigma \end{cases}$$

The PS model in the high-temperature, high-density limit



$$T^* \rightarrow \infty \Rightarrow x \approx T^{*-1} \rightarrow 0$$

Only "chain" diagrams survive!

A non-trivial result is obtained in the high-density limit:

$$\rho \rightarrow \infty, \hat{\rho} \equiv \rho x = \text{finite}$$

The PS model in the high-temperature, high-density limit

$$\lim_{\substack{x \rightarrow 0 \\ \rho \rightarrow \infty \\ \hat{\rho} = \rho x}} y(r) = 1 + x \sum_{n=1}^{\infty} \hat{\rho}^n \text{---} \overset{n}{\circ} \text{---} \bullet \text{---} \dots \text{---} \bullet \text{---} \circ$$

$$= 1 + xw(r)$$

$$\tilde{w}(k) = \sum_{n=1}^{\infty} \hat{\rho}^n [\tilde{f}_{\text{HS}}(k)]^{n+1} = \hat{\rho} \frac{[\tilde{f}_{\text{HS}}(k)]^2}{1 - \hat{\rho} \tilde{f}_{\text{HS}}(k)}$$

$$\lim_{\substack{x \rightarrow 0 \\ \rho \rightarrow \infty \\ \hat{\rho} = \rho x}} S(k) = \frac{1}{1 - \hat{\rho} \tilde{f}_{\text{HS}}(k)}$$

Thermodynamic quantities

L. Acedo, A. Santos / Physics Letters A 323 (2004) 427–433

Contributions of zeroth- and first-order in x to the main thermodynamic quantities

Quantity	$\mathcal{O}(x^0)$	$\mathcal{O}(x)$	
(excess) free energy/particle pressure	$a_{\text{ex}}/k_B T$	$2^{d-1} \hat{\eta}$	$2^{d-1} \gamma(\sigma)$
(excess) entropy/particle	$p/\rho k_B T$	$1 + 2^{d-1} \hat{\eta}$	$2^{d-1} \hat{\eta} w(\sigma)$
(excess) chemical potential	s_{ex}/k_B	0	$2^{d-1} \hat{\eta} [w(\sigma) - \frac{1}{2}]$
(excess) internal energy/particle	$\mu_{\text{ex}}/k_B T$	$2^d \hat{\eta}$	$2^{d-1} [\hat{\eta} - 2^{-d} w(0)]$
(excess) specific heat	$u_{\text{ex}}/k_B T$	$2^{d-1} \hat{\eta}$	$2^{d-2} [\hat{\eta} - 2^{1-d} w(0)]$
(inverse) isothermal compressibility	c_{ex}/k_B	0	$\frac{1}{2} \hat{\eta} \partial w(0) / \partial \hat{\eta}$
	$(\partial p / \partial \rho)_T / k_B T$	$1 + 2^d \hat{\eta}$	$2^{d-1} \partial [\hat{\eta}^2 w(\sigma)] / \partial \hat{\eta}$

$$\tilde{\gamma}(k) = -\hat{\eta} \tilde{f}_{\text{HS}}(k) - v_d \sigma^d \ln [1 - \hat{\rho} \tilde{f}_{\text{HS}}(k)]$$

$$\hat{\eta} = \hat{\rho} v_d \sigma^d: \text{ scaled packing fraction}$$

$$v_d = (\pi/4)^{d/2} / \Gamma(1 + d/2)$$

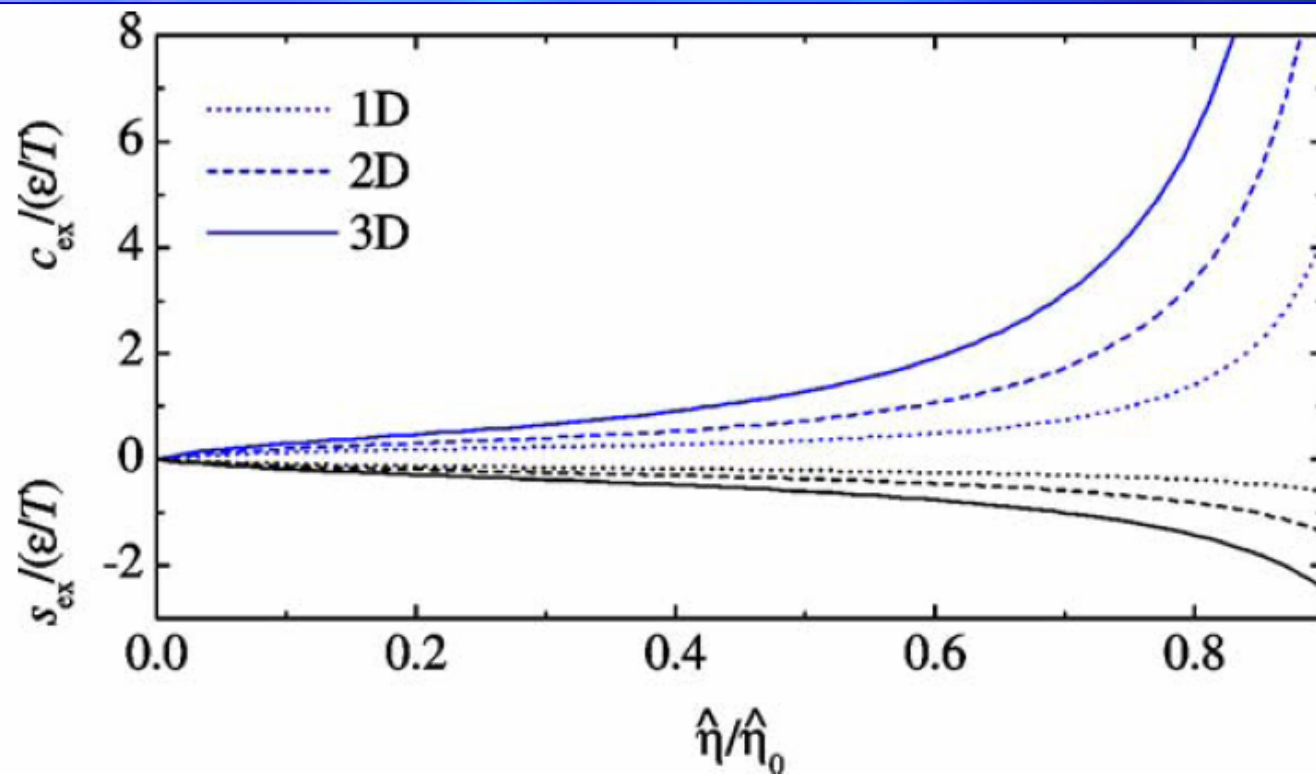


Fig. 1. Plot of $s_{\text{ex}}/(\epsilon/T)$ (lower curves) and $c_{\text{ex}}/(\epsilon/T)$ (upper curves) versus $\hat{\eta}/\hat{\eta}_0$ for $d = 1$ (dotted lines), $d = 2$ (dashed lines) and $d = 3$ (solid lines).

$\hat{\eta} \rightarrow \hat{\eta}_0$



Spinodal instability

Spinodal instability

$$S(k) = \frac{1}{1 - \hat{\rho} \tilde{f}_{\text{HS}}(k)}$$

$$\tilde{f}_{\text{HS}}(k) = \tilde{f}_{\text{max}} \text{ at } k = k_0$$

$$S(k_0) \rightarrow \infty \text{ when } \hat{\rho} \rightarrow \hat{\rho}_0 \equiv 1/\tilde{f}_{\text{max}}$$

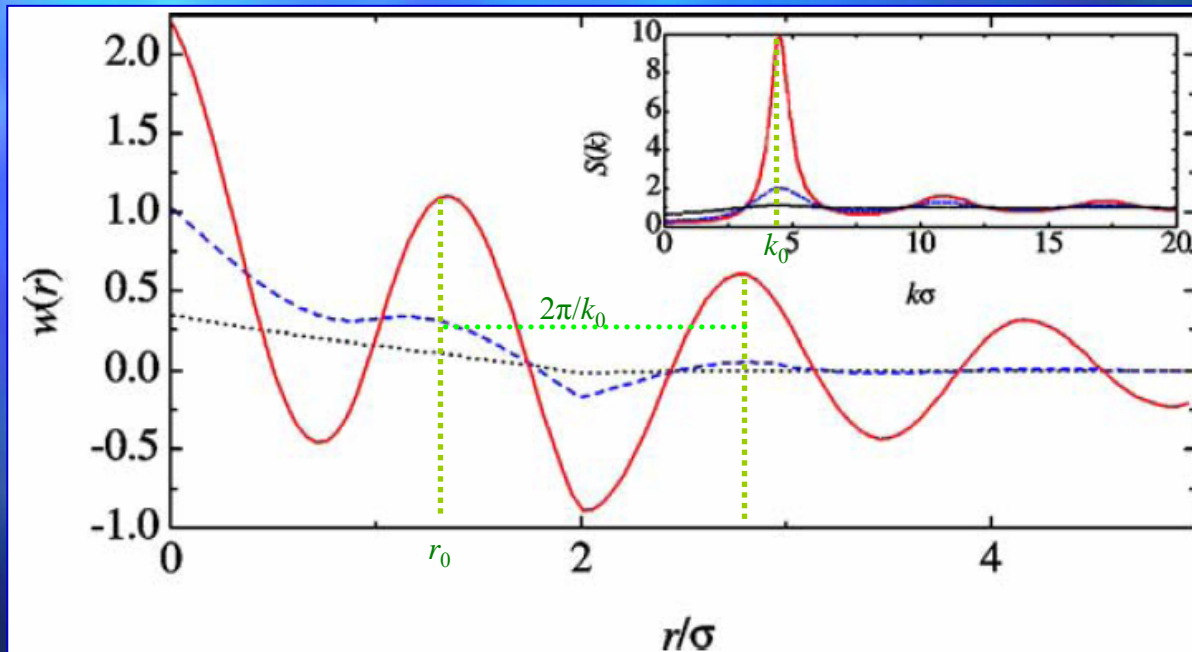


Fig. 2. Plot of $w(r)$ and $S(k)$ (see inset) at $\hat{\eta}/\hat{\eta}_0 = 0.1$ (dotted lines), 0.5 (dashed lines) and 0.9 (solid lines) for $d = 1$.

L. Acedo, A. Santos / Physics Letters A 323 (2004) 427–433

Table 2

Values of the HS close-packing fraction η_{cp} , the wavenumber k_0 , the nearest-neighbor distance r_0 , the (scaled) spinodal instability packing fraction $\hat{\eta}_0$, the (scaled) freezing packing fraction $\hat{\eta}_f$, the (scaled) packing fraction $\hat{\eta}_{\text{ms}}$ at the condition of marginal stability and the (scaled) melting packing fraction $\hat{\eta}_m$

d	η_{cp}	$k_0\sigma$	r_0/σ	$\hat{\eta}_0$	$\hat{\eta}_f$	$\hat{\eta}_{\text{ms}}$	$\hat{\eta}_m$
1	1	4.49	1.40	2.30	1.00	1.00	1.00
2	$\sqrt{3}\pi/6 \simeq 0.91$	5.14	1.37	1.89	0.89	0.95	1.03
3	$\sqrt{2}\pi/6 \simeq 0.74$	5.76	1.34	1.45	0.62	0.69	0.80
4	$\pi^2/16 \simeq 0.62$	6.38	1.32	1.07	0.36	0.41	0.50
5	$\sqrt{2}\pi^2/30 \simeq 0.47$	6.99	1.30	0.76	0.22	0.26	0.33

“Critical” behavior:

correlation length: $\xi \sim (1 - \hat{\eta}/\hat{\eta}_0)^{-1/2}$

$$w(r) \sim (1 - \hat{\eta}/\hat{\eta}_0)^{-1/2} (k_0 r)^{-(d-1)/2} \cos[k_0 r - (d-1)\pi/4]$$

- The PS *fluid* ceases to exist (even in 1D!) in the high-temperature limit when

$$\hat{\rho} \equiv \rho x \geq \hat{\rho}_0 (\Rightarrow \hat{\eta} \equiv \eta x \geq \hat{\eta}_0)$$

- The *freezing* transition must occur at a smaller value of the (scaled) packing fraction:

$$\hat{\eta}_f \leq \hat{\eta}_{ms} \leq \hat{\eta}_m < \hat{\eta}_0$$

freezing

marginal
stability

melting

A simple picture of the PS solid at high temperature

- Lattice sites occupied by “clusters” of overlapping spheres (α/x spheres/site).
- Every cluster behaves as a hard-core super-particle.
- Packing fraction of clusters: $\eta/(\alpha/x)$.

$$u_{\text{ex}}^{\text{solid}}/k_B T = \alpha/2$$

$$s_{\text{ex}}^{\text{solid}}/k_B T = -d \ln \left[1 - (\hat{\eta}/\alpha\eta_{\text{cp}})^{1/d} \right] - d \ln 2 \quad (\text{Free volume theory})$$

α : variational parameter to minimize the free energy

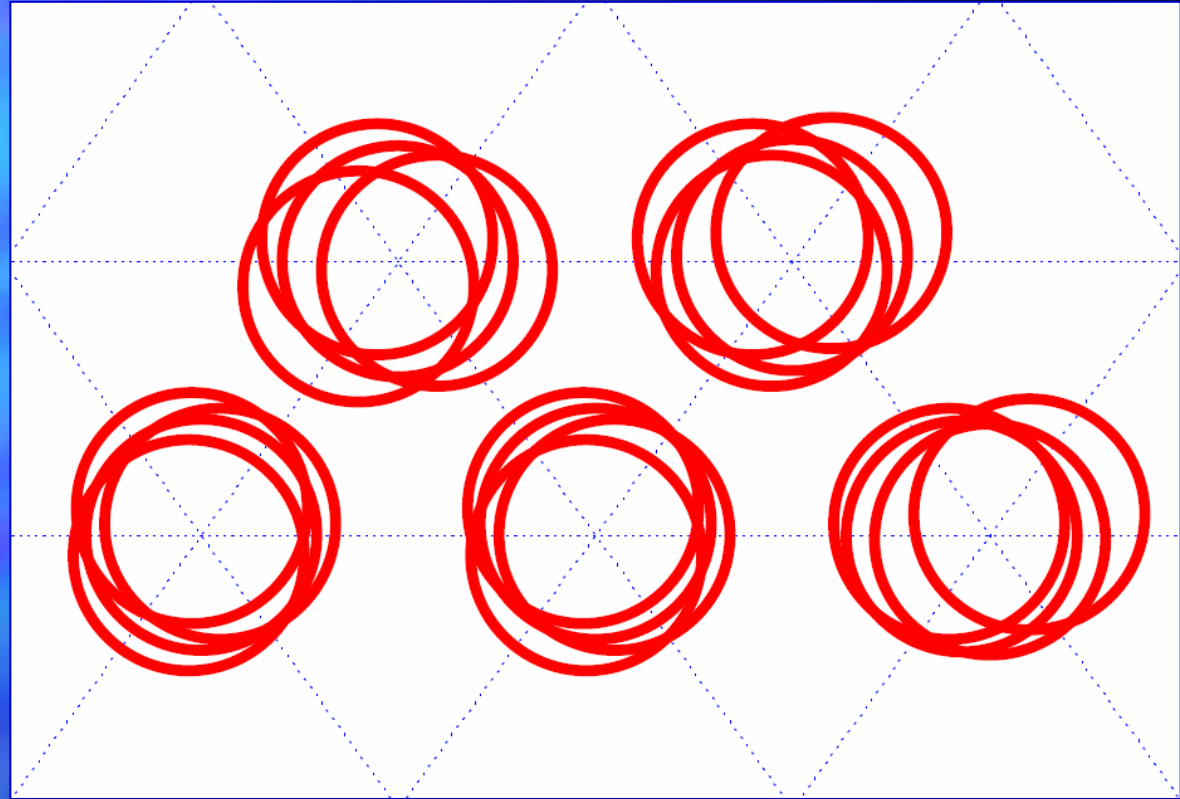


Table 2

Values of the HS close-packing fraction η_{cp} , the wavenumber k_0 , the nearest-neighbor distance r_0 , the (scaled) spinodal instability packing fraction $\hat{\eta}_0$, the (scaled) freezing packing fraction $\hat{\eta}_f$, the (scaled) packing fraction $\hat{\eta}_{ms}$ at the condition of marginal stability and the (scaled) melting packing fraction $\hat{\eta}_m$

d	η_{cp}	$k_0\sigma$	r_0/σ	$\hat{\eta}_0$	$\hat{\eta}_f$	$\hat{\eta}_{ms}$	$\hat{\eta}_m$
1	1	4.49	1.40	2.30	1.00	1.00	1.00
2	$\sqrt{3}\pi/6 \simeq 0.91$	5.14	1.37	1.89	0.89	0.95	1.03
3	$\sqrt{2}\pi/6 \simeq 0.74$	5.76	1.34	1.45	0.62	0.69	0.80
4	$\pi^2/16 \simeq 0.62$	6.38	1.32	1.07	0.36	0.41	0.50
5	$\sqrt{2}\pi^2/30 \simeq 0.47$	6.99	1.30	0.76	0.22	0.26	0.33

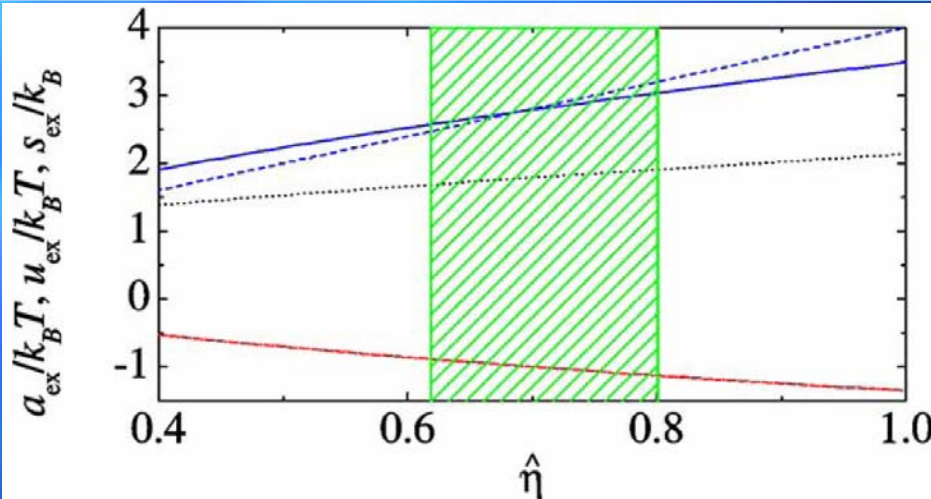


Fig. 3. Excess free energy per particle in the three-dimensional PS solid, $a_{ex}^{solid}/k_B T$ (solid line), and PS fluid, $a_{ex}^{fluid}/k_B T$ (dashed line), in the high-temperature limit. The excess internal energy, $u_{ex}^{solid}/k_B T$ (dotted line), and the excess entropy, $s_{ex}^{solid}/k_B T$ (dashed-dotted line), of the PS solid are also plotted. The shaded area represents the fluid-solid coexistence region.

Outline

- Effective interactions in colloidal dispersions. The penetrable-sphere (PS) model.
- A few (general) statistical-mechanical definitions.
- Exact properties of the PS fluid in the high-temperature limit. Spinodal instability.
- The high-T approximation.
- The low-T approximation (1D).
- Comparison with MC simulations (1D).
- Conclusions.

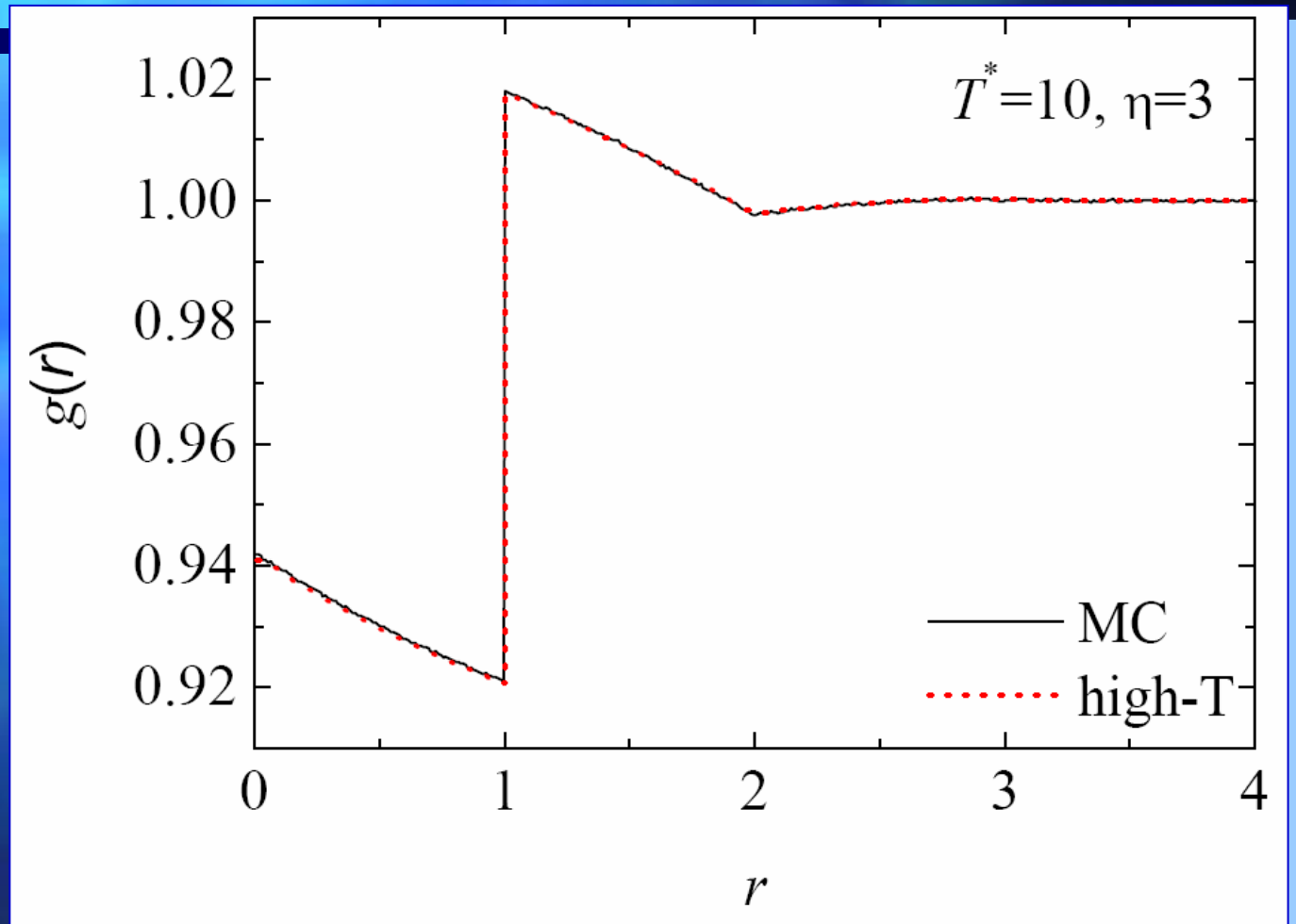
High-temperature (HT) *approximation*

$$\lim_{\substack{x \rightarrow 0 \\ \rho \rightarrow \infty \\ \hat{\rho} = \rho x}} y(r|\rho, T) = 1 + xw(r|\hat{\rho}), \quad x \equiv 1 - e^{-1/T^*}$$

$$y_{\text{HT}}(r|\rho, T) = \frac{1}{1 - xw(r|\rho x)}$$

$$g_{\text{HT}}(r|\rho, T) = \begin{cases} (1 - x)y_{\text{HT}}(r|\rho, T), & r < \sigma \\ y_{\text{HT}}(r|\rho, T), & r > \sigma \end{cases}$$

Test of the high-T approximation (1D)



Outline

- Effective interactions in colloidal dispersions. The penetrable-sphere (PS) model.
- A few (general) statistical-mechanical definitions.
- Exact properties of the PS fluid in the high-temperature limit. Spinodal instability.
- The high-T approximation.
- The low-T approximation (1D).
- Comparison with MC simulations (1D).
- Conclusions.

Towards a low-temperature (LT) approximation (1D)

Some exact properties:

$$G(t) \equiv \int_0^{\infty} dr g(r) e^{-rt} = \frac{1}{\rho} \frac{P(t)}{1 - P(t)}$$

Laplace transform of the nearest neighbor distribution: $P(t)$

- $P(t) = 1 - \frac{1}{\rho}t + O(t^2)$
- $\lim_{\rho \rightarrow 0} y(r) = 1 \Rightarrow \lim_{\rho \rightarrow 0} P(t)/\rho = \frac{1-x+xe^{-t}}{t}$
- $\lim_{T^* \rightarrow 0} P(t) = \frac{\xi e^{-t}}{t+\xi}$ (hard rods)

Low-temperature (LT) approximation (1D)

First step:

$$P(t) = \frac{\gamma + \xi_2 e^{-t}}{t + \xi_1}, \quad \xi_1 = \frac{1 - \rho}{\rho}(1 - \gamma), \quad \xi_2 = \xi_1 - \gamma$$

$$g(r) = \sum_{n=0}^{\infty} f_n(r - n) \Theta(r - n), \quad f_n(r) = \frac{\xi_2^n e^{-\xi_2 r} r^{n-1}}{\rho n!} (n + \gamma r)$$

$$y(\sigma^-) = y(\sigma^+) \Rightarrow \left(e^{1/T^*} - 1 \right) e^{-\xi_2 \gamma} = \xi_2$$

Low-temperature (IT) approximation (1D)

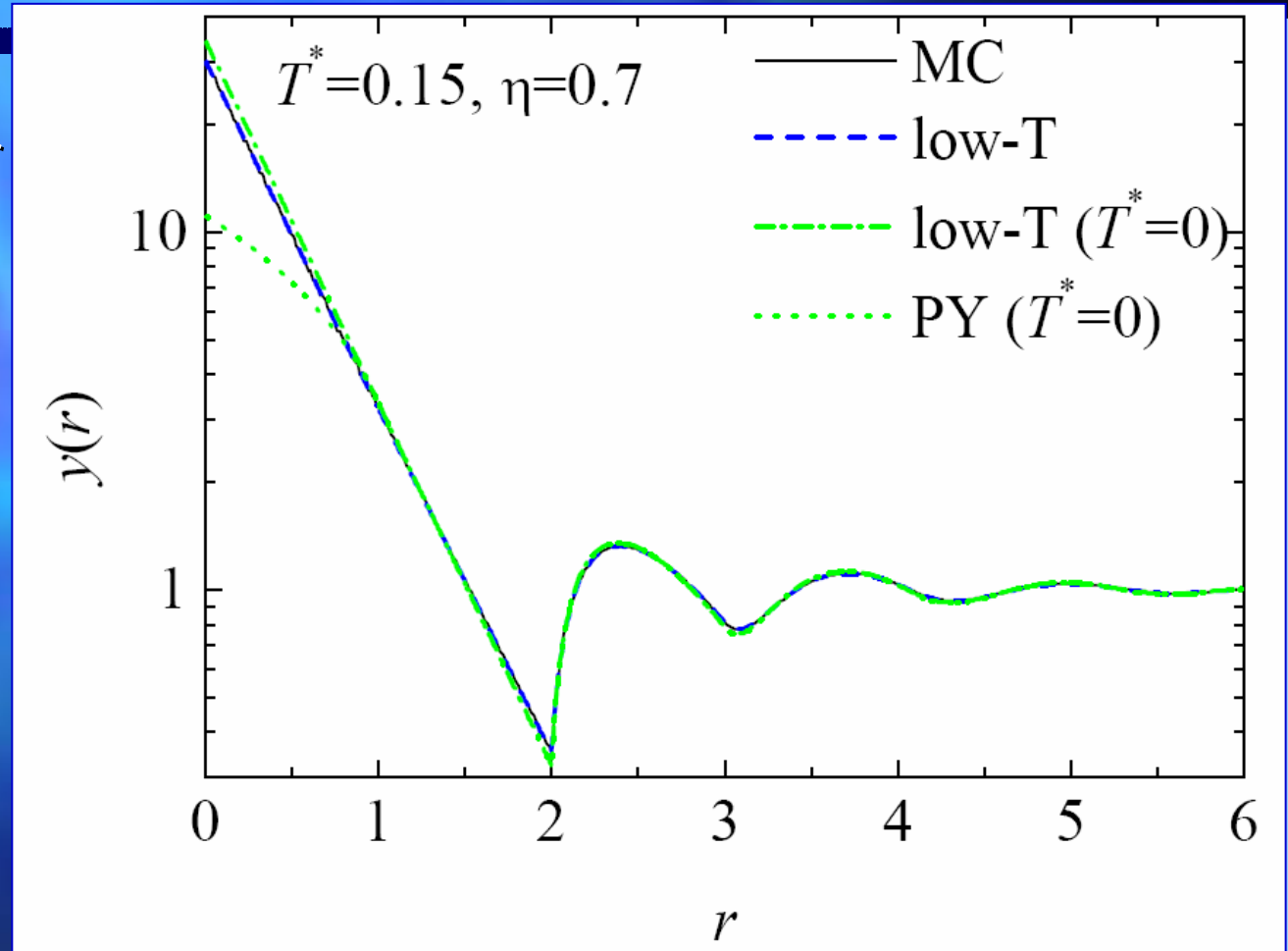
Second step:

$$g_{\text{LT}}(r) = \sum_{n=0}^{\infty} f_n(r-n)\Theta(r-n) + (r-1)A\Theta(1-r)$$

$$y'(\sigma^-) = y'(\sigma^+) \Rightarrow A = e^{-1/T^*} \frac{\gamma \xi_2}{\rho}$$

Test of the low-T approximation (1D)

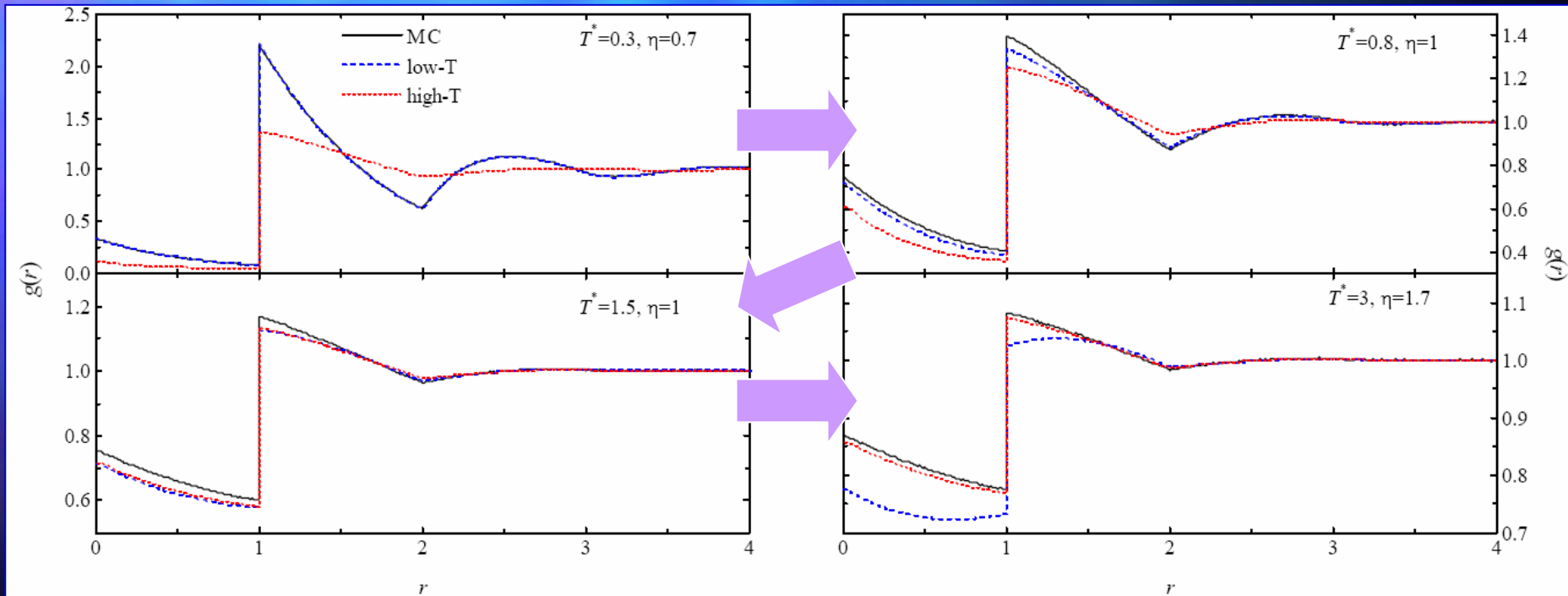
The PY theory for hard rods is not exact for $r < \sigma$!



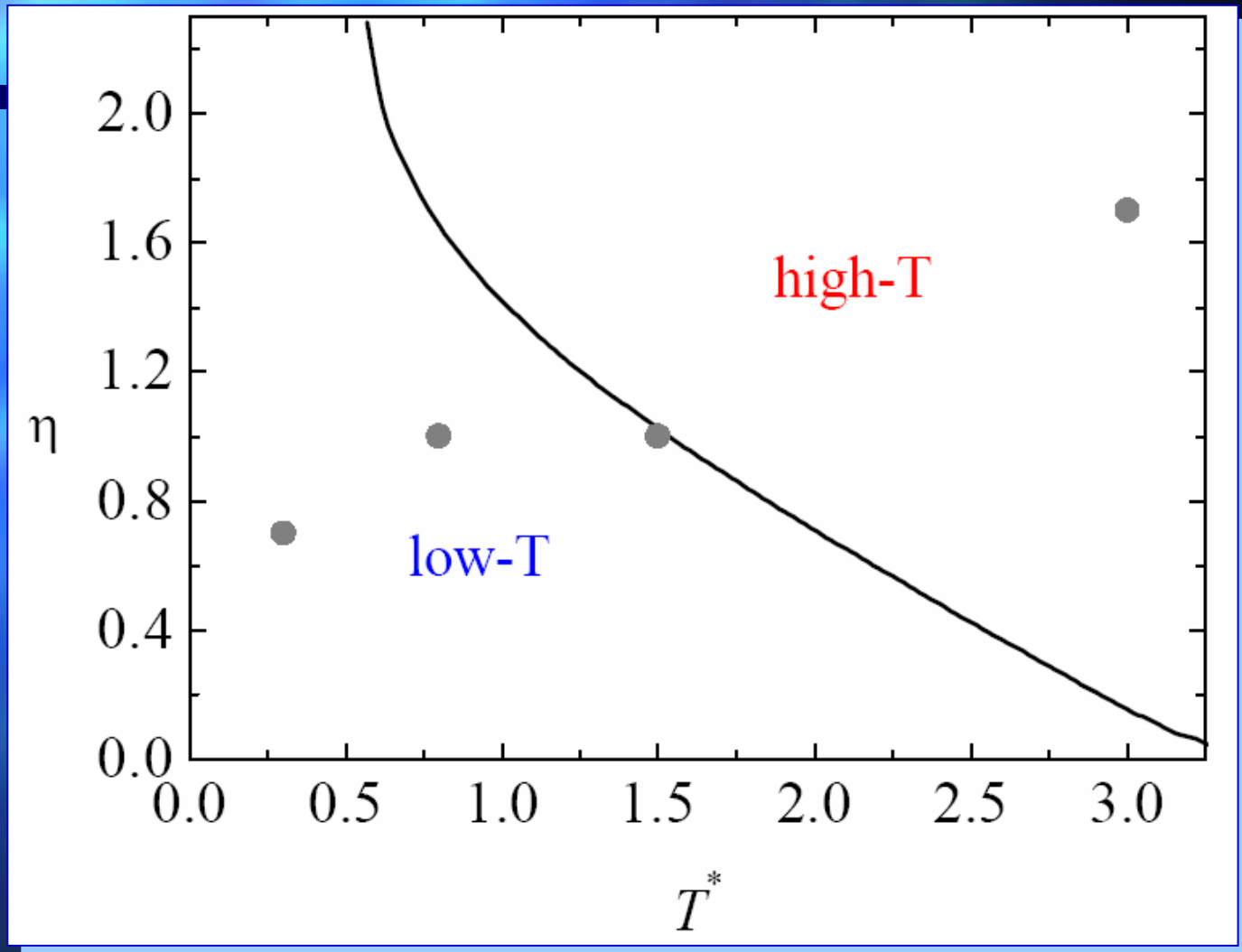
Outline

- Effective interactions in colloidal dispersions. The penetrable-sphere (PS) model.
- A few (general) statistical-mechanical definitions.
- Exact properties of the PS fluid in the high-temperature limit. Spinodal instability.
- The high-T approximation.
- The low-T approximation (1D).
- Comparison with MC simulations (1D).
- Conclusions.

Comparison between MC simulations and the HT and LT approximations (1D)



"Basins" of the high-T and low-T approximations



Conclusions (I)

- Apart from its practical interest in soft matter, the PS model is theoretically interesting: it represents a crossover between hard spheres (low temperatures) and the ideal gas (high temperatures).
- The structural and thermodynamic functions can be *exactly* derived in the combined high-temperature, high-density limit.
- The fluid presents a spinodal instability at an upper bound density $\eta_0(T^*) \sim T^*$, but this is preempted by a first-order phase transition to the solid at the freezing density $\eta_f(T^*) \sim T^*$.

Conclusions (II)

- An extrapolation of the asymptotic high-T results to finite temperatures provides a good approximation for moderate and high temperatures, as shown by comparison with 1D simulations.
- The above approximation is complemented by a low-T approximation that reduces to the exact results for hard rods in the zero-temperature limit.
- Extension of the above approaches to the 3D case is under current investigation.

THANKS!

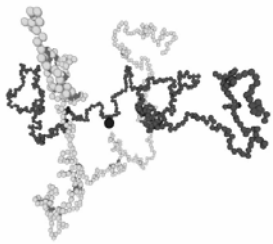


Fig. 14. A snapshot from a simulation involving two self-avoiding polymers. In this configuration, the centers of mass of the two chains (denoted by the big sphere) coincide, without violation of the excluded-volume conditions. (Courtesy of Arben Jusufi.)

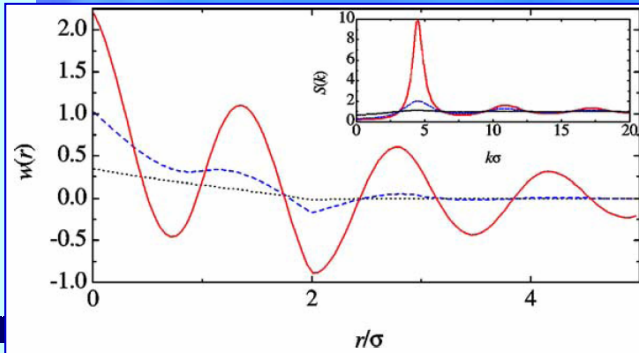
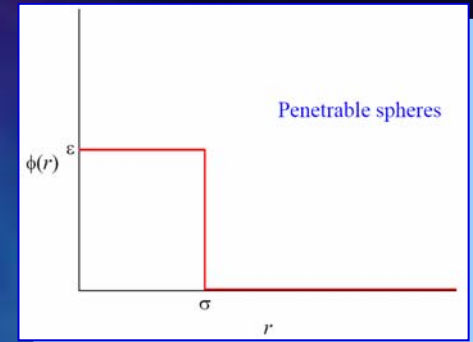


Fig. 2. Plot of $w(r)$ and $S(k)$ (see inset) at $\hat{\eta}/\hat{\eta}_0 = 0.1$ (dotted lines), 0.5 (dashed lines) and 0.9 (solid lines) for $d = 1$.

